Chaotic pulse transmission and spiral formation in a calcium oscillation model

H. Sakaguchi[1] and P. Woafo[2]
[1]*Department of Applied Science for Electronics and Materials, Interdisciplinary Graduate School of Engineering Sciences, Kyushu University, Kasuga, Fukuoka 816-8580, Japan*
[2]*Laboratory of Nonlinear Modeling and Simulation in Engineering and Biological Physics, Faculty of Science, University of Yaounde I, P.O. Box 812, Yaounde, Cameroon*
(Received 29 October 2007; published 23 April 2008)

We study a two-dimensional reaction-diffusion equation for calcium oscillation with a pacemaker region. When the pacemaker entrains the whole system, circular waves are observed as a target pattern. However, if the pace of the pacemaker is too fast, the pulse propagation to the outer region sometimes fails in a chaotic manner. We find that spiral waves are spontaneously created at the interface between the pacemaker region and the outer region.

DOI: 10.1103/PhysRevE.77.042902 PACS number(s): 87.18.−h, 05.45.Xt

Spiral waves in oscillatory and excitatory media are found in various systems such as the Belousov-Zhabotinskii reaction, cellular slime molds [1], oscillatory oxidation of carbon monoxide on a Pt(110) surface [2], and ventricular tachycardia [3]. In the problem of cardiac dynamics, spiral formation leads to serious irregular pulse, and it is important to understand the mechanism of the spiral formation. Several mechanisms to generate spirals are known. In the Belousov-Zhabotinskii reaction, spirals are generated when a piece of a quasi-one-dimensional pulse is cut by stirring the solution locally or light impulse [4]. A spiral is created when the waves surround a sharp edge [5]. In these cases, wave propagation is stable. On the other hand, if some kinds of instability such as the lateral instability or the alternans instability occur in quasi-one-dimensional traveling pulses or the meandering instability occurs strongly in a single spiral, many spiral pairs can be spontaneously created, which leads to spiral chaos [6–8]. In this paper, we report another mechanism of spiral formation: i.e., spiral formation at the interface between a pacemaker region and an outer region. Spirals are not successively created like the case of spiral chaos, because the quasi-one-dimensional pulse propagates stably in the outer region. The failure of the frequency locking or the desynchronization between the pacemaker region and the outer region plays an essential role for the spiral formation.

We will show the spiral formation at the interface between the pacemaker region and the outer region in a model of Ca^{2+} waves. The calcium ion (Ca^{2+}) is one of the most versatile and universal signaling agents in biological processes from fertilization, cell proliferation, muscle contraction, and synaptic plasticity and apoptosis, and Ca^{2+} oscillation plays important roles in some of those processes [9]. It is considered that some information such as strength of input signal is encoded in the frequency of the Ca^{2+} oscillation and transmitted as the Ca^{2+} wave. Intracellular Ca^{2+} waves were observed first in medaka eggs [10] and then observed in various cells such as epithelial cells [11], astrocytes syncitium [12], and endothelium cells [13]. Spiral waves were observed in Xenopus oocytes [14] and hippocampal slice cultures [15]. Spatiotemporal organization by Ca^{2+} dynamics from the subcellular to organ level was reviewed by Dupont *et al.* [16]. A number of theoretical models for the Ca^{2+} oscillation have been proposed, and the numerical simulations have been performed [17]. Falcke *et al.* found spiral breakup and spiral chaos [18] and localized spiral waves owing to the dispersion gap in a model of Ca^{2+} oscillation [19].

In this paper, we use one of the simplest models proposed by Dupont *et al.* [20]. There are intracellular Ca^{2+} pools (ER) in a cell. The uptake and release of Ca^{2+} from the Ca^{2+} store is controlled by cytosolic Ca^{2+} concentration. The Ca^{2+}-induced Ca^{2+} release can occur by a positive feedback at the Ca^{2+} store. Two variables—the cytosolic Ca^{2+} concentration X and the calcium concentration Y of the internal store (ER)—are used in the model. The model equations are written as

$$\frac{dX}{dt} = V_0 + k_f Y - kX - V_1(X,Y) + V_2(X,Y),$$

$$\frac{dY}{dt} = V_1(X,Y) - V_2(X,Y) - k_f Y, \tag{1}$$

where V_0 is a steady flow of Ca^{2+} to the cytosol, $-kX$ denotes the uptake from the cytosol, $V_1(X,Y)$ denotes active uptake of Ca^{2+} from the cytosol to the internal store, $V_2(X,Y)$ denotes active release of Ca^{2+} from the internal store to the cytosol, and $k_f Y$ is a diffusional flow of Ca^{2+} from the internal store to the cytosol. The active flows are assumed to take the form

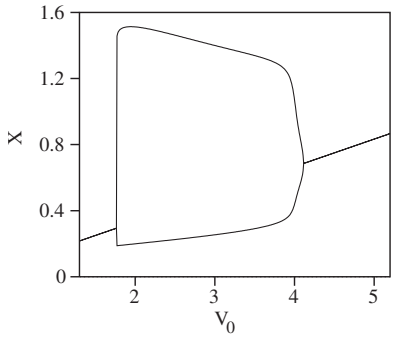

FIG. 1. Maximum and minimum values of X as V_0 is changed.

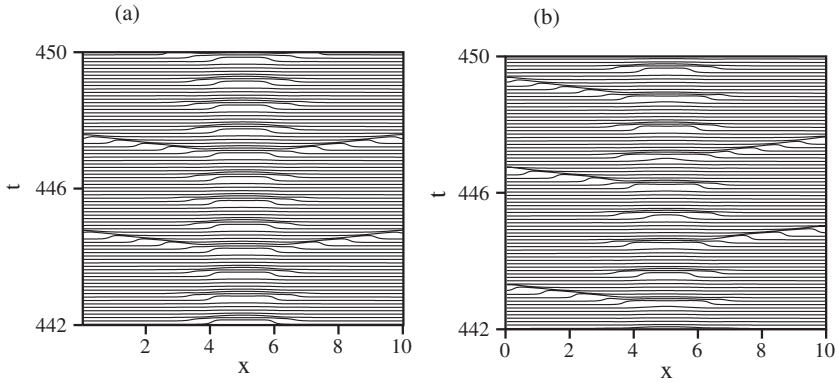

FIG. 2. Time evolution of $X(x,t)$ for (a) $a_0=2.6$ and (b) $a_0=2$.

$$V_1(X,Y) = \frac{V_{1m}X^2}{k_2^2 + X^2},$$

$$V_2(X,Y) = \frac{V_{2m}X^4Y^2}{(k_a^4 + X^4)(k_r^2 + Y^2)}. \quad (2)$$

The parameter values are set to be $k_f=2$, $k=6$, $V_{1m}=65$, $V_{2m}=500$, $k_2=1$, $k_a=0.9$, and $k_r=2$ in this paper. We have performed numerical simulation from an initial condition $X=0.2$ and $Y=0.2$ to show it. Figure 1 displays the maximum and minimum values of X during the time evolution, as V_0 is changed. The limit cycle oscillation of Ca^{2+} appears for $1.77 < V_0 < 4.11$.

Kepseu and Woafo studied a discretely coupled one-dimensional model and found irregular oscillation [21]. We study one- and two-dimensional models for the calcium oscillation. The model equation is

$$\frac{\partial X}{\partial t} = V_0 + a(x,y) + k_f Y - kX - V_1(X,Y) + V_2(X,Y) + D\nabla^2 X,$$

$$\frac{\partial Y}{\partial t} = V_1(X,Y) - V_2(X,Y) - k_f Y, \quad (3)$$

where $V_0=1.3$ and $a(x,y)$ denotes spatially dependent steady flow of Ca^{2+}. We have assumed a diffusion-type coupling. The diffusion coefficient D is set to be 1. We have numerically calculated with a finite-difference method of time step Δt and grid size Δx. If the grid size Δx is not so small, the model is interpreted as a discretely coupled system, but in this paper, we use a rather small value $\Delta x=0.02$ and it is a good approximation to the reaction-diffusion equations (3). For time evolution, we have used the Runge-Kutta method with $\Delta t=2.5\times 10^{-5}$.

First, we show the numerical results of one-dimensional simulations. The system size is $L_x=10$, and no-flux boundary conditions are used. The spatially dependent input $a(x)$ is $a(x)=a_0$ for $L_x/2-1<x<L_x/2+1$ and $a(x)=0$ for $x>L_x/2+1, x<L_x/2-1$. The central region $L_x/2-1<x<L_x/2+1$ plays the role of pacemaker if $0.47<a_0<2.81$. The outer regions $x<L_x/2-1$ and $x>L_x/2+1$ act as excitable media. Figures 2(a) and 2(b) display the time evolutions of $X(x)$ for (a) $a_0=2.6$ and (b) $a_0=2$. In the pacemaker region, the Ca^{2+} oscillation appears. The periodic stimuli from the pacemaker region excite the outer regions, but the pulse propagation succeeds only once in a while. The pulse propagation passes through the outer regions every four times of the oscillation in the central pacemaker region at $a_0=2.6$; that is, the 4:1 frequency locking is attained between the pacemaker region and the outer regions. The pulse propagation occurs irregularly every three or four times of the oscillation in the central pacemaker region at $a_0=2$. We call this phenomenon chaotic pulse transmission. The pulse propagation is not synchronized for both sides of the central pacemaker region, because which pulses are successfully transmitted to the outer regions are different on the two sides, although they are emitted at the same time from the center. Figures 3(a) and 3(b) display time evolutions of $X(x,t)$ at $x=L_x/2$ and $L_x/5$. The time evolution at $x=L_x/2$ exhibits regular limit-cycle oscillation. However, the time evolution is irregular and sporadic at $x=L_x/5$ owing to the chaotic pulse transmission.

We have calculated the first Lyapunov exponent as a measure of chaos from the following linearized equation of Eqs. (3):

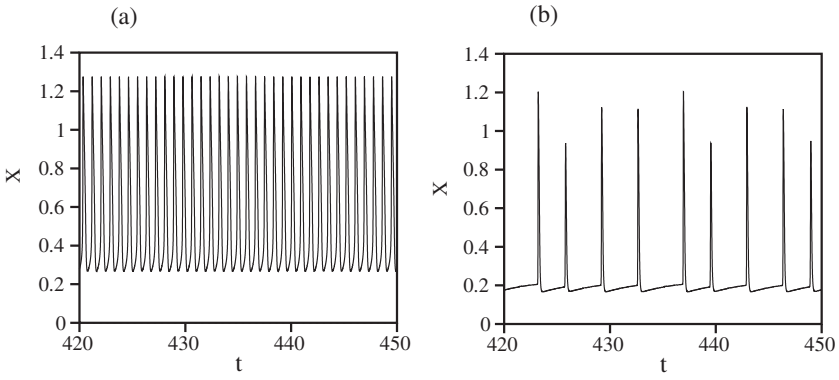

FIG. 3. (a) Time evolution of $X(x,t)$ at $x=L_x/2$ for $a_0=2$. (b) Time evolution of $X(x,t)$ at $x=L_x/5$ for $a_0=2$.

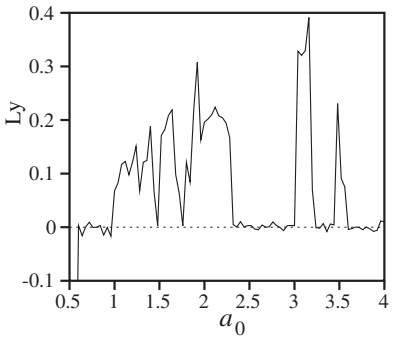

FIG. 4. The first Lyapunov Ly exponent calculated by using Eq. (4).

$$\frac{\partial \delta X}{\partial t} = k_f \delta Y - k \delta X - V_{1X}(X,Y)\delta X - V_{1Y}(X,Y)\delta Y + V_{2X}(X,Y)\delta X + V_{2Y}(X,Y)\delta Y + D\partial^2 \delta X/\partial x^2,$$

$$\frac{\partial \delta Y}{\partial t} = V_{1X}(X,Y)\delta X + V_{1Y}(X,Y)\delta Y - V_{2X}(X,Y)\delta X - V_{2Y}(X,Y)\delta Y - k_f \delta Y, \quad (4)$$

where $V_{1X}=\partial V_1(X,Y)/\partial X$, $V_{1Y}=\partial V_1(X,Y)/\partial Y$, $V_{2X}=\partial V_2(X,Y)/\partial X$, and $V_{2Y}=\partial V_2(X,Y)/\partial Y$. The first Lyapunov exponent is calculated as the time average of the linear growth rate of the norm $\{\int dx(|\delta X|^2+|\delta Y|^2)\}^{1/2}$. Figure 4 displays the first Lyapunov exponent as a function of a_0. The Lyapunov exponent is positive at $a_0=2$, and it is almost zero at $a_0=2.6$, which is consistent with the time evolutions shown in Fig. 2.

Next, we study pulse propagation in two dimensions. No-flux boundary conditions are assumed at the boundaries. The system size is $L_x \times L_y$, where L_x is fixed to be 10 and L_y is changed as a control parameter. First, we consider a quasi-one-dimensional system. That is, $a(x,y)$ take $a_0=2$ in a linear banded region $L_x/2-1<x<L_x/2+1$ and $a(x,y)$ is 0 in the other region. The chaotic pulse transmission in the one-dimensional system implies whether the pulse transmission occurs or not is different at each position of y if the coupling in the y direction does not exist. On the other hand, the diffusion coupling tends to make the pulse propagation uniform. There is a kind of competition between the chaotic pulse transmission and the uniform pulse propagation. The uniform pulse propagation is represented by a special one-dimensional solution which satisfies $X(x,y)=X_0(x)$ and $Y(x,y)=Y_0(x)$. The pulse propagation is synchronized in the y direction in this solution. We can study the linear stability of the special solution by assuming that $X(x,y)=X_0(x)+\delta X(x,y)$ and $Y(x,y)=Y_0(x)+\delta Y(x,y)$. The perturbations take the form of a linear combination of the Fourier modes $\delta X=\delta X_k(x,t)\sin\{k(y-L_y/2)\}$ and $\delta Y=\delta Y_k(x,t)\sin\{k(y-L_y/2)\}$ with $k=(2n-1)\pi/L_y$ or $\delta X=\delta X_k(x,t)\cos\{k(y-L_y/2)\}$ and $\delta Y=\delta Y_k(x,t)\cos\{k(y-L_y/2)\}$ with $k=2n\pi/L_y$ owing to the no-flux boundary conditions. The Fourier amplitudes δX_k and δY_k obey

$$\frac{\partial \delta X_k}{\partial t} = k_f \delta Y_k - k \delta X_k - V_{1X}(X,Y)\delta X_k - V_{1Y}(X,Y)\delta Y_k + V_{2X}(X,Y)\delta X_k + V_{2Y}(X,Y)\delta Y_k + D\partial^2 \delta X_k/\partial x^2 - Dk^2 \delta X_k,$$

$$\frac{\partial \delta Y_k}{\partial t} = V_{1X}(X,Y)\delta X_k + V_{1Y}(X,Y)\delta Y_k - V_{2X}(X,Y)\delta X_k - V_{2Y}(X,Y)\delta Y_k - k_f \delta Y_k. \quad (5)$$

The stability exponent or the transverse Lyapunov exponent can be calculated as the time average of the linear growth rate of the norm $\{\int dx(|\delta X_k|^2+|\delta Y_k|^2)\}^{1/2}$. Figure 5(a) is the stability exponent as a function of $L=\pi/k$. The stability exponent takes positive values for $L=\pi/k>2.25$. If the system size L_y in the y direction is smaller than 2.25, the perturbations with wave number $k=\pi/L_y$ in the y direction are expected to decay. On the other hand, for $L_y>2.25$, the perturbations in the y direction grow and the uniform pulse propagation becomes unstable. Figure 5(b) displays a snapshot pattern for $L_y=2$. The pulse is propagating only in the $-x$ direction. The flat one-dimensional pulse is stable against the perturbation in the y direction, because L_y is sufficiently small. On the other hand, Fig. 5(c) displays a snapshot pattern for $L_y=8$. The flat one-dimensional pulse becomes unstable in this wider system. The pulse propagation is success-

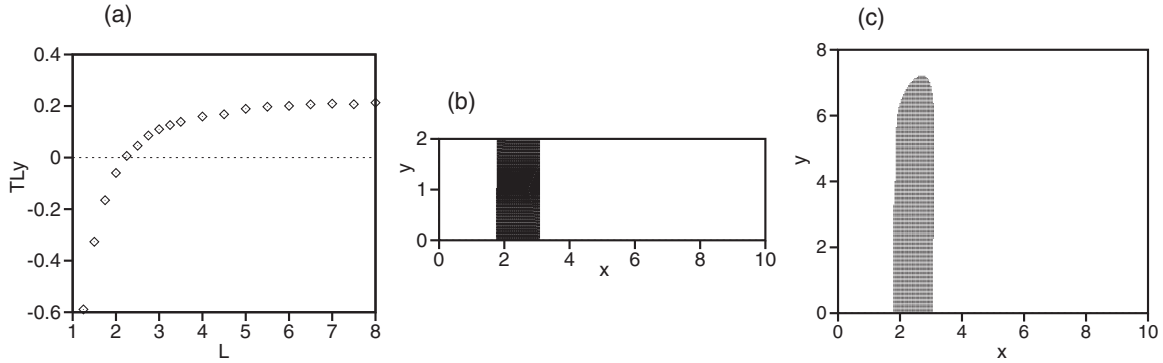

FIG. 5. (a) Stability exponent TLy as a function of $L=\pi/k$ for a system with a linear pacemaker region calculated by using Eq. (5). (b) One-dimensional pulse for $L_y=2$, which is propagating in the $-x$ direction. In the shaded region, $X>0.5$. (c) Traveling pulse with an end point as a result of the lateral instability for $L_y=8$. In the shade region, $X>0.5$.

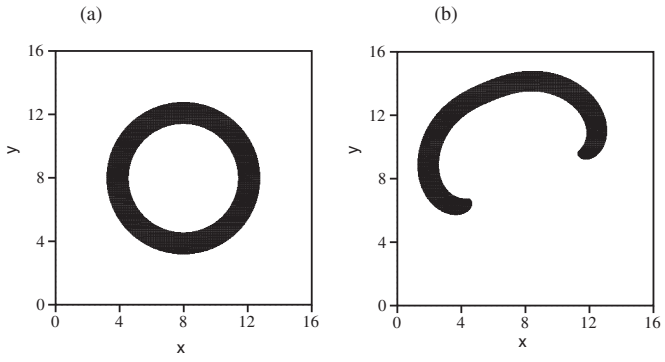

FIG. 6. Snapshot patterns in a two-dimensional system with a circular pacemaker region with radius (a) $r_0=1$ and (b) $r_0=2$. In the shaded region, $X>0.5$.

ful for $y<7$, but the pulse propagation has failed for $y>7$. As a result of the desynchronization, a pulse with an end point appears and it leads to the spiral formation. Even if desynchronization occurs, the flat one-dimensional pulse can propagate, if the $n:1$ entrainment occurs completely between the pacemaker region and the outer regions and the chaotic behavior does not appear [22]. We have checked it for the parameter value $a_0=2.6$. Desynchronization and the resultant chaotic pulse transmission are necessary conditions for our phenomenon,

We have also performed of a numerical simulation of a purely two-dimensional system, where $a(x,y)$ takes a nonzero value $a(x,y)=a_0=2$ in $r<r_0$ where $r=\sqrt{(x-L_x/2)^2+(y-L_y/2)}$. In the outer region of $r>r_0$, $a(x,y)$ is set to be 0. The radius r_0 of the pacemaker region is changed as a control parameter. The system size is $L_x\times L_y=16\times 16$, and the no-flux boundary conditions are imposed. Figure 6(a) displays a snapshot pattern at $r_0=1$. (In the shaded region, $X<0.5$.) In this case, the pulse propagation is synchronized and circular waves propagate outwards. The curvature effect works in the two-dimensional system with a small pacemaker region in contrast to the quasi-one dimensional system shown in Fig. 5. Figure 6(b) displays snapshot patterns for $r_0=2$. The circular waves become unstable and the pulse propagates only locally from the pacemaker region toward the outer region. In other words, the pulse transmission toward the outer region is successful in some sector, but it fails in the other sector. The partial pulse transmission leads to the formation of a pair of spirals. If the radius of the pacemaker region is even larger, the circular pulse is broken up into many wavelets at the interface, which grow to many pairs of spirals. The spiral waves are stable in the outer region and no more spirals are further created in the outer regions, which is qualitatively different from the case of spiral chaos.

To summarize, we have found a mechanism of spiral generation at the interface between a pacemaker region and an outer region owing to the chaotic pulse transmission at the interface. The chaotic pulse transmission might be controlled and can be used as an encoder of information, although biological evidence for this is not known. We have studied a model of Ca^{2+} oscillation in this paper, but the phenomenon is considered to be general, and we would like to study this phenomenon also in other systems.

[1] A. T. Winfree, *The Geometry of Biological Time* (Springer-Verlag, New York, 1980).
[2] S. Jakubith, H. H. Rotermund, W. Engel, A. von Oertzen, and G. Ertl, Phys. Rev. Lett. **65**, 3013 (1990).
[3] F. X. Witkowski, L. J. Leon, P. A. Penkoske, W. R. Giles, M. L. Spano, W. L. Ditto, and A. T. Winfree, Nature (London) **392**, 78 (1998).
[4] A. V. Panfilov and B. N. Vasiev, Physica D **49**, 107 (1991).
[5] M. Gómez-Gesteira, J. L. del Castillo, M. E. Vázquez-Iglesias, V. Pérez-Munuzuri, and V. Pérez-Villar, Phys. Rev. E **50**, 4646 (1994).
[6] M. Bär and M. Eiswirth, Phys. Rev. E **48**, R1635 (1993).
[7] A. V. Panfilov, Phys. Rev. Lett. **88**, 118101 (2002).
[8] H. Sakaguchi and T. Fujimoto, Phys. Rev. E **67**, 067202 (2003).
[9] M. J. Berridge, M. D. Bootman, and P. Lipp, Nature (London) **395**, 645 (1998).
[10] E. B. Ridgway, J. C. Gilkey, and L. F. Jaffe, Proc. Natl. Acad. Sci. U.S.A. **74**, 623 (1977).
[11] M. J. Sanderson, A. C. Charles, and E. R. Dirksen, Cell Regul. **1**, 585 (1990).
[12] A. H. Cornell-Bell, S. M. Finkbeiner, M. S. Cooper, and S. J. Smith, Science **247**, 470 (1990).
[13] T. R. Uhrenholt, T. L. Domeier, and S. S. Segal, Am. J. Physiol. Heart Circ. Physiol. **292**, H1634 (2007).
[14] J. Lechleiter, S. Girard, E. Peralta, and D. Clapham, Science **252**, 123 (1991).
[15] M. E. Harris-White, S. A. Zanotti, S. A. Frautschy, and A. C. Charles, J. Neurophysiol. **79**, 1045 (1998).
[16] G. Dupont, L. Combettes, and L. Leybaert, Int. Rev. Cytol. **261**, 193 (2007).
[17] M. Falcke, Adv. Phys. **53**, 255 (2004).
[18] M. Falcke, M. Bär, J. D. Lechleiter, and J. L. Hudson, Physica D **129**, 236 (1999).
[19] M. Falcke, M. Or-Guil, and M. Bär, Phys. Rev. Lett. **84**, 4753 (2000).
[20] G. Dupont, A. Goldbeter, and M. J. Berridge, Cell Regul. **1**, 853 (1990).
[21] W. D. Kepseu and P. Woafo, Phys. Rev. E **73**, 041912 (2006).
[22] H. Sakaguchi and T. Fujimoto, Prog. Theor. Phys. **108**, 241 (2002).